



OPEN Chronic stress in adulthood results in microvascular dysfunction and subsequent depressive-like behavior

Xiaochen Zhang^{1,2,3}, Yaru Wang^{1,2,3}, Song Xue^{1,2}, Li Gong^{1,2}, Jinglan Yan^{1,2}, Yuanjia Zheng^{1,2}, Xiaoyun Yang^{1,2}, Yujing Fan¹, Kuizhang Han¹, Yongjun Chen^{1,2}✉ & Lin Yao^{1,2}✉

Depression is a prevalent mental disorder characterized by unknown pathogenesis and challenging treatment. Recent meta-analyses reveal an association between cardiovascular risk factors and an elevated risk of depression. Despite this, the precise role of vascular injury in depression development remains unclear. In this investigation, we assess vascular system function in three established animal models of depression—chronic unpredictable mild stress (CUMS), chronic social defeat stress (CSDS) and maternal separation (MS)—utilizing ultrasonography and laser Doppler measurement. All three model animals exhibit anhedonia and despair-like behavior. However, significant microvascular dysfunction (not macrovascular) is observed in animals subjected to CUMS and CSDS models, while such dysfunction is absent in the MS model. Statistical analysis further indicates that microcirculation dysfunction is not only associated with depression-like behavior but is also intricately involved in the development of depression in the CUMS and CSDS models. Furthermore, our study has proved for the first time that endothelial nitric oxide synthase-deficient (*eNOS*^{+/-}) mice, which is a classic model of vascular endothelial injury, showed depression-like behavior which occurred two months later than microvascular dysfunction. Notably, the mitigation of microvascular dysfunction successfully reverses depression-like behavior in *eNOS*^{+/-} mice by enhancing nitric oxide production. In conclusion, this study unveils the pivotal role of microvascular dysfunction in the onset of depression induced by chronic stress in adulthood and proposes that modulating microvascular function may serve as a potential intervention in the treatment of depression.

Keywords Microvascular dysfunction, Depressive animal model, *eNOS*^{+/-} mice, NO production

Depression, affecting one in five individuals during their lifetime, stands as the leading cause of disabilities worldwide¹. While current mainstream treatments predominantly target the nervous system, first-line drugs, including serotonin-norepinephrine reuptake inhibitors, selective serotonin-reuptake inhibitors, and ketamine, manifest notable side effects such as slow onset time², high addiction potential³, and hallucinogenic properties⁴. Exploring avenues beyond the central nervous system may offer safer and more effective approaches for depression interventions⁵. Clinical studies reveal a higher incidence of depression in individuals with cardiovascular or circulatory system diseases, like stroke^{6,7}. Magnetic resonance imaging (MRI) examinations in depressed patients indicate abnormal cerebral microvascular and endothelial cell function^{8,9}. Classic vascular disease treatments, such as Statins, show significant antidepressant effects, linked to improved blood-brain barrier permeability and endothelial cell function¹⁰. Furthermore, some animal studies explore the molecular relationship between vascular injury and depression; for instance, chronic restraint stress increases serum vascular endothelial growth factor levels in mice¹¹, and unpredictable chronic mild stress elevates serum concentrations of intercellular adhesion molecule-1, vascular cell adhesion molecule-1, and matrix metalloproteinase-9 in mice¹². Despite these efforts, the role of vascular injury in depression development and treatment remains unclear.

Cerebral microvascular, an integral component of the neurovascular unit, sustains the brain's normal physiological function and features prominently in research on various diseases, including dementia, Alzheimer's

¹Research Institute of Acupuncture and Moxibustion, Shandong University of Traditional Chinese Medicine, Jinan 250355, People's Republic of China. ²Innovative Institute of Chinese Medicine and Pharmacy, Shandong University of Traditional Chinese Medicine, Jinan 250355, People's Republic of China. ³These authors contributed equally: Xiaochen Zhang and Yaru Wang. ✉email: chen Yongjun@sduatcm.edu.cn; yaolin@sduatcm.edu.cn

disease, and depression¹³. Damage to cerebral microvasculature is closely linked to impaired neural network functions such as synaptic pruning and synapse formation¹⁴. Nitric oxide (NO), an endothelial vasodilator, produced by endothelial nitric oxide synthase (*eNOS*) through hydrolyzing L-arginine in vascular endothelial cells, plays a vital role in maintaining vascular function and barrier integrity¹⁵. NO is implicated in various brain pathologies, including vascular dementia¹⁶, Alzheimer's disease¹⁷ and stroke¹⁸. Clinical research consistently reports reduced plasma levels of NO metabolites in depression patients¹⁹. The classic model of endothelial cell injury in the vascular system, *eNOS* knockout mice, exhibits diverse phenotypes of microvascular damage, including spontaneous cerebral small-vessel disease²⁰, glomerular capillary damage²¹ and cardiac microvascular damage²². Recent studies indicate that these mice spontaneously exacerbate vascular endothelial injury with age²³, potentially leading to symptoms of neurodegenerative diseases such as dementia²⁴. Understanding the intricate relationship between vascular injury and depression at the molecular level is imperative for advancing our comprehension of depression etiology and refining treatment strategies.

Stress emerges as a pivotal factor contributing to the manifestation of depressive disorders²⁵. Clinical investigations have demonstrated a connection between stress and the development of vascular dysfunction, hypertension, atherosclerosis, and various circulatory system diseases²⁶. Three prevalent rodent models, namely chronic unpredictable mild stress (CUMS), chronic social defeat stress (CSDS), and maternal separation (MS), are established to mimic depressive disorders. These models involve diverse pathogenic stimuli such as changeable and unpredictable stress, chronic social stress, and early life stress, respectively²⁷. Previous studies have indicated that animals subjected to stress-induced depression exhibit an increased susceptibility to cardiovascular diseases, linked to autonomic dysfunction, abnormal oxidative stress levels, and endothelial dysfunction^{28–31}. However, a comprehensive investigation into the relationship between vascular function and depression within these frequently used animal models is currently lacking.

In our study, we assessed vascular function in the aforementioned three classic depression animal models using ultrasonography and laser Doppler measurement. We conducted a thorough analysis of the correlation between circulation and depressive disorder symptoms through correlation and mediation analyses. Additionally, we utilized *eNOS*^{+/-} mice to ascertain the impact of vascular damage on the onset of depression and explored whether the restoration of vascular dysfunction could reverse depression-like behavior in these mice. This study aims to provide compelling evidence for the critical role of vascular injury in the development of diverse stress-induced depressions, advocating for the vascular system as a potential target in the treatment of depression.

Result

Chronic stress in adulthood cause microvascular dysfunction

To investigate the impact of different stress types on depressive disorders, we initially employed three widely used animal models for experimental studies: the CUMS model, CSDS model, and MS model (Supplementary Fig. 2A). Following exposure to stress stimuli, depressive-like behavior was assessed through two kinds of behavior tests. The open field test (OFT) gauged locomotor activity and general mental state, while the sucrose preference test (SPT) and forced swimming test (FST) determined the presence of depressive-like behavior. As depicted in Supplementary Fig. 2B–D, CUMS and CSDS stimuli significantly decreased locomotor activity in the OFT in mice compared to their respective control groups. Concurrently, mice from CUMS and CSDS models displayed reduced time in the OFT center, indicative of heightened anxiety states. Conversely, no differences in locomotor activity and time in the OFT center were observed between MS rats and their controls. Furthermore, animals exposed to CUMS, CSDS, and MS stimuli exhibited a significantly lower percentage of sucrose consumption during SPT and an increase in the duration of immobility time during FST compared to their respective controls (Supplementary Fig. 2E and F). These findings affirm the successful induction of depressive-like behavior in rodents through the three distinct stimuli.

We investigated the presence of microvascular dysfunction in animal models of depression induced by three types of stress. Using laser Doppler, we assessed the microvascular status of various body parts, including the average perfusion unit (PU) values of the meninx, right forepaw, and right hindpaw. Microvascular function was further evaluated by determining the post-occlusive reactive hyperemia (PORH) time of the right hindpaw. In comparison with their respective control groups, mice exposed to CUMS and CSDS exhibited a significant decrease in PU values for the meninx, right forepaw, and right hindpaw (Fig. 1A–F). Additionally, these three types of stress increased the PORH time in the right hindpaw of mice (Fig. 1G and H). Interestingly, no marked differences were observed in PU values for different body parts and the PORH time of the right hindpaw in MS rats compared with their controls (Fig. 1A–H). These findings suggest that exposure to CUMS and CSDS during adulthood can lead to microvascular system damage and impair small vessel function, while early-life stress such as MS does not have these effects.

Stress does not cause macrocirculatory system disorder

To further assess the impact of the three types of stress on the macrocirculatory system, we analyzed cardiac function in animals from each stress model (Supplementary Fig. 3A and B). Echocardiographic measurements were used to evaluate parameters such as Ejection Fraction (EF), Fractional Shortening (FS), Stroke Volume (SV), Left Ventricular Internal Dimension in Systole (LVIDs), and Left Ventricular Posterior Wall in Systole (LVPWs). No significant changes were observed in EF, FS, SV, LVIDs, and LVPWs in any of the models compared with their respective control groups (Supplementary Fig. 3C–G). To further investigate the effects of the three types of stress on arterial function, ultrasound was utilized to measure peak systolic blood flow velocity in arteries of different body parts, including the aortic arch (AOA), left common carotid artery (LCCA), abdominal aorta (AA), and left femoral artery (LFA). No noticeable changes were observed in the systolic peak flow velocity of AOA (Fig. 2A–C), LCCA (Fig. 2D–F), AA (Fig. 2G–I), and LFA (Fig. 2J–L) between control and model animals from each type of stress. These results indicate that the three types of stressors investigated had no discernible

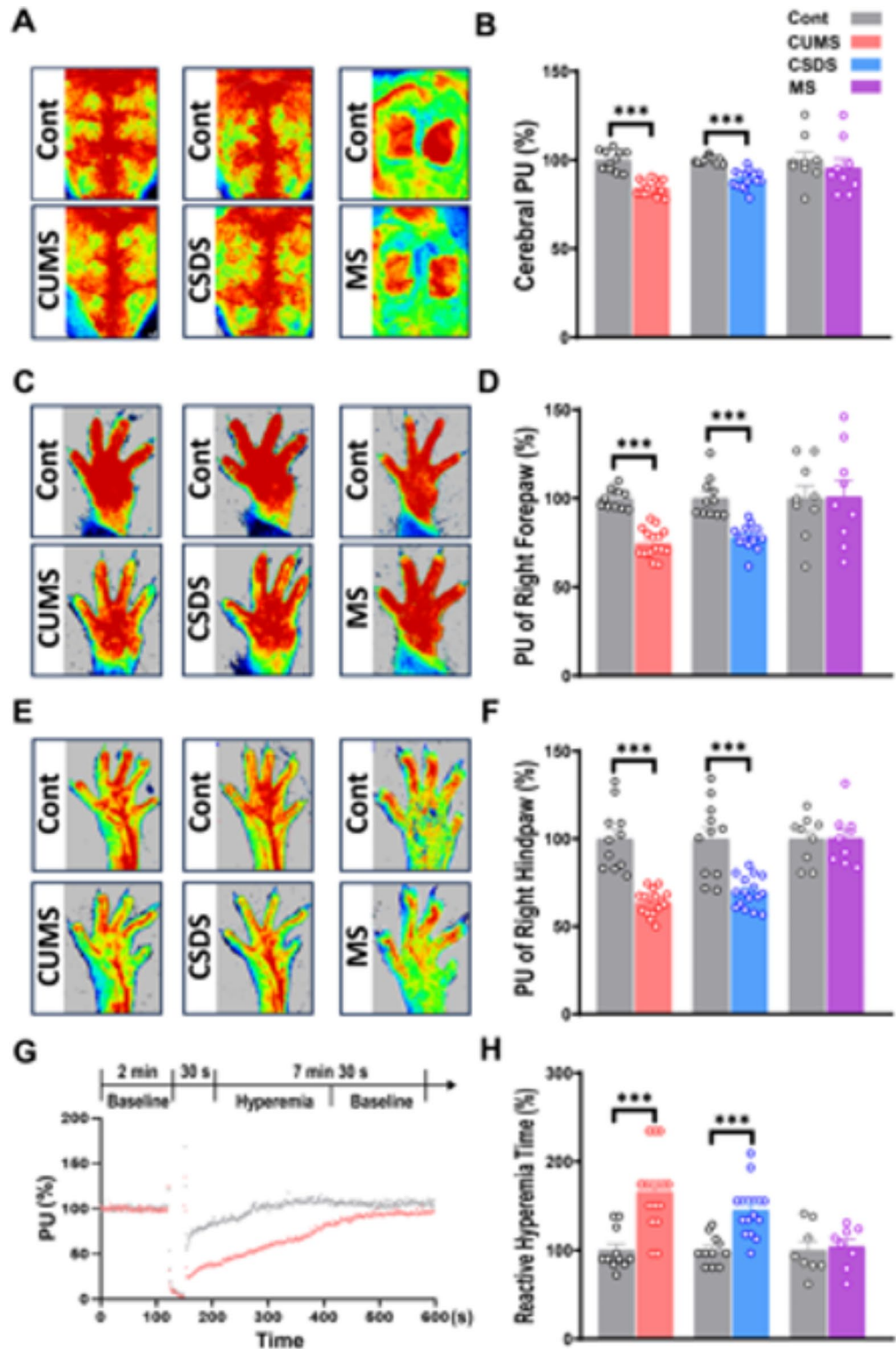


Fig. 1. Different types of stress lead to microvascular dysfunction. (A) Representative laser speckle images of cerebral perfusion in each group; (B) Standardized statistical results of cerebral PU in each group; (C) Representative laser speckle images of right forepaw perfusion in each group; (D) Standardized statistical results of right forepaw PU in each group; (E) Representative laser speckle images of right hindpaw perfusion in each group; (F) Standardized statistical results of right hindpaw PU in each group; (G) Schematic diagram of the PORH test; (H) Standardized statistical results of PORH time in each group; PU: Perfusion Unit. Control group was used as the standard value (100%) in each group. $P^* < 0.05$, $P^{**} < 0.01$, $P^{***} < 0.001$ vs. Control.

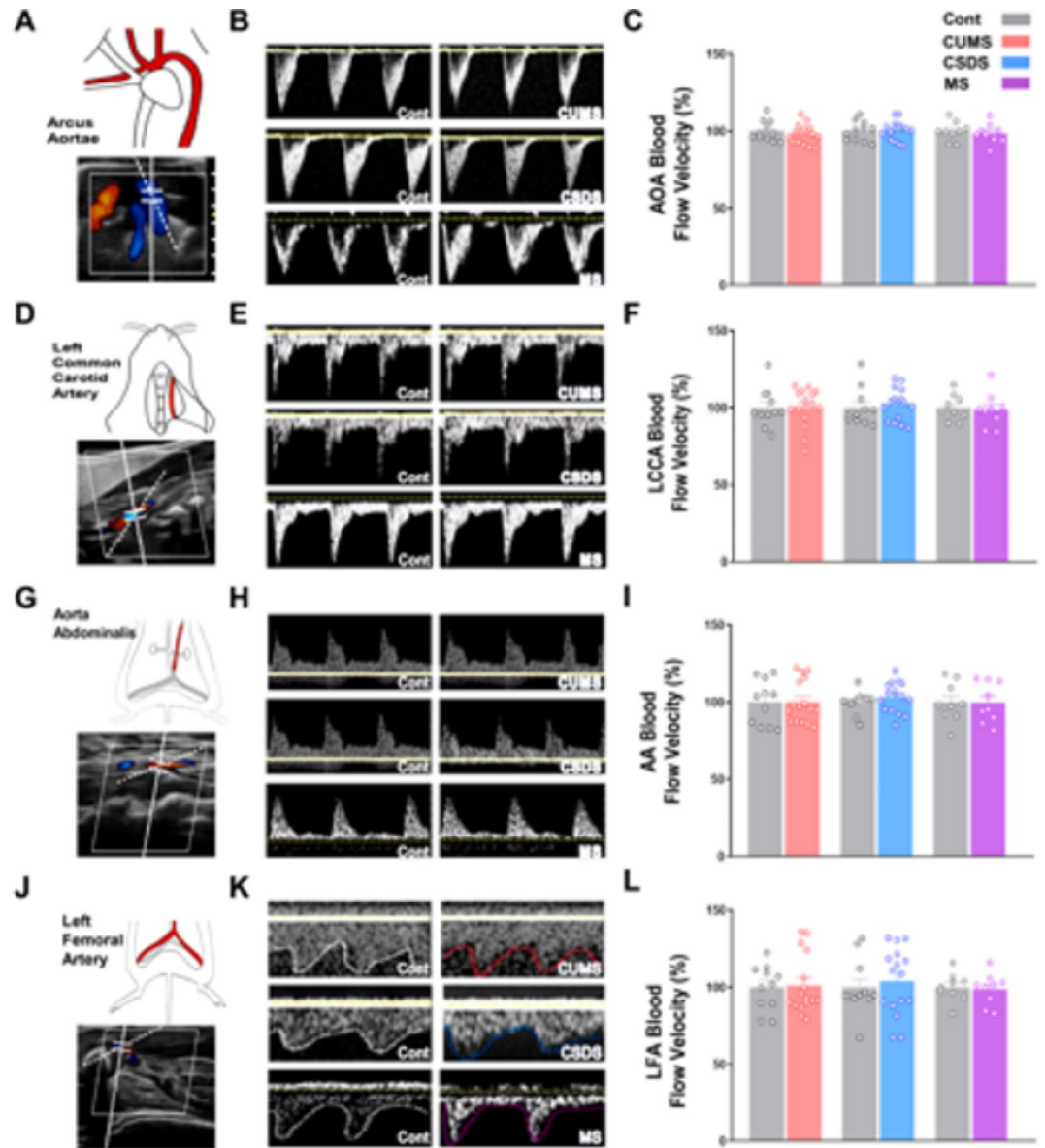


Fig. 2. Different types of stress did not cause macro-circulatory system disorder. (A) Schematic diagram of the experiment and representative ultrasonography images of the AOA in B-Mode. (B) Representative ultrasonography images of the AOA in M-Mode. (C) Standardized statistical results of peak systolic blood flow velocity in AOA of each model. (D) Schematic diagram of the experiment and representative ultrasonography images of the LCCA in B-Mode. (E) Representative ultrasonography images of the LCCA in M-Mode. (F) Standardized statistical results of peak systolic blood flow velocity in LCCA of each model. (G) Schematic diagram of the experiment and representative ultrasonography images of the AA artery in B-Mode. (H) Representative ultrasonography images of the AA in M-Mode. (I) Standardized statistical results of peak systolic blood flow velocity in AA of each model. (J) Schematic diagram of the experiment and representative ultrasonography images of the LFA artery in B-Mode. (K) Representative ultrasonography images of the LFA in M-Mode. (L) Standardized statistical results of peak systolic blood flow velocity in LFA of each model. LCCA: Left Common Carotid Artery; AOA: Aortic Arch; AA: Abdominal Aorta; LFA: Left Femoral Artery. Control group was used as the standard value (100%) in each group.

impact on the functions of the heart and arteries, suggesting the absence of macrocirculatory system disorders in animals exposed to CUMS, CSDS, and MS.

Mediating effect of microvascular dysfunction on chronic stress-induced depression-like behavior in adulthood

To investigate the potential association between circulatory damage and stress-induced depressive disorder, we performed Spearman correlation analysis on all symptom evaluation indicators within the variable range. In the CUMS model, a significant correlation was observed between microvascular evaluation variables (meninx

microvascular perfusion, right forepaw and right hindpaw microvascular perfusion, and the time of post-occlusive reactive hyperemia) and depressive-like behavior (sucrose preference and immobility time during forced swimming). Figure 3A and B presents the Spearman correlation coefficients and a heatmap illustrating the relationship between each variable. These findings highlight a positive correlation between microvascular evaluation variables and sucrose preference, while indicating a negative correlation with the immobility time during forced swimming. Notably, variables related to cardiac function (ejection fraction, fractional shortening, stroke volume, left ventricular internal diameter in systole, and left ventricular posterior wall thickness in systole) and macro-circulation system function (systolic velocity of aortic arch, left common carotid artery, abdominal aorta, and left femoral artery) showed no significant correlation with depressive-like behavior. Similar results were obtained in CSDS model (Supplementary Fig. 4A and B). These results collectively suggest a positive correlation between microvascular dysfunction and anhedonia, as well as a negative correlation with behavioral despair induced by CUMS and CSDS.

To further elucidate the pivotal role of microvascular dysfunction in the onset and progression of depressive disorder, we employed “microvascular dysfunction” as a potential mediator for mediation analysis between stress factors and core symptoms of depression-like behavior. The results indicate that microvascular dysfunction resulting from CUMS contributes to both anhedonia and behavioral despair. The indirect effects on anhedonia and behavioral despair were 49.111% (95% CI: -0.635, -0.209) and 54.569% (95% CI: 0.113, 0.786), respectively (Fig. 3C and D). In CSDS, microvascular dysfunction was partially involved in the development of anhedonia by 22.694% (95% CI: -0.356, -0.037), whereas the mediating effect on behavioral despair was not significant (Supplementary Fig. 4C and D). These findings underscore the crucial role of microvascular disturbances in the chronic stress models (CUMS and CSDS) leading to depressive behavior, while indicating that it is not the primary cause in the development of depression induced by early life stress (MS).

Microvascular dysfunction in *eNOS*^{+/-} mice results in depression-like behavior

To substantiate the critical role of microvascular dysfunction in the development of depression, we employed a transgenic mouse model with partial deficiency in expressing *eNOS*^{+/-}. This mouse model has been unequivocally identified as exhibiting microvascular and vascular endothelial cell dysfunction³². Initially, to assess the onset of microvascular damage, the emergence of depression-like behavior, and the progression of these phenotypes, we monitored microvascular perfusion in the meninx, right forepaw, and right hindpaw, as well as the PORH times of the right hindpaw every two months from birth in *eNOS*^{+/-} mice and their littermates (Fig. 4A). Laser Doppler measurements revealed that, compared with wild-type littermates, *eNOS*^{+/-} mice exhibited significantly decreased PU at all testing locations starting at two months of age (Fig. 4B-D). Additionally, the PORH time was notably increased, indicating impaired microvascular function in *eNOS*^{+/-} mice at this age (Fig. 4E). Behavioral test results demonstrated that a partial deficiency in the *eNOS* gene did not alter the total distance covered in the open field test at each time point (data unshown). However, *eNOS*^{+/-} mice exhibited a lower percentage of sucrose preference and an increase in immobility time during forced swimming starting from 4 months of age, which was 2 months later than the initial detection of microvascular damage (Fig. 4F-H). These findings also proved that the extent of microvascular injury and depression-like behavior in *eNOS*^{+/-} mice progressively worsened with aging (Fig. 4H).

The improvement of microvascular dysfunction rescues depression-like behaviors in *eNOS*^{+/-} mice

To further investigate the link between microvascular dysfunction and depression-like behaviors, we utilized arginase inhibitors to enhance the bioavailability of L-arginine to *eNOS* in mice, thereby boosting NO production. At 4 months of age, we screened *eNOS*^{+/-} mice with microvascular dysfunction accompanied by depressive behavior, the mice were treated with arginase inhibitors (Nor-NOHA, 10 mg/kg, i.p.) once every 2 days for a total of 6 weeks (Fig. 5A). Initially, compared with littermate controls, the reduced PU value of the right hindpaw in *eNOS*^{+/-} mice was completely reversed after 4 weeks of Nor-NOHA treatment, indicating the recovery of impaired microvascular function (Fig. 5B). However, the degree of sucrose preference significantly increased to control level until 6 weeks of drug treatment compared with *eNOS*^{+/-} mice (Fig. 5C). Consequently, we selected 6 weeks as the total treatment time. Subsequently, we evaluated microvascular function and depression-like behavior after 6 weeks of Nor-NOHA administration. Notably, depression-like behavior in *eNOS*^{+/-} mice was completely restored, as indicated by the elevated percentage of sucrose consumption and the decreased immobility time in the forced swimming test (Fig. 5C and D). In addition, NO production in brain tissue was successfully restored to wild type control level after 6-week Nor-NOHA treatment, which is accompanied with the increased cerebral vascular perfusion and reduced PORH time in the right hindpaw in *eNOS*^{+/-} mice (Fig. 5E - G), suggesting that regulation of NO level and alleviation of microvascular dysfunction are the basis for the improvement of depression-like behaviors in the condition of *eNOS* gene deficiency. These results further confirm the pivotal role of microvascular function in the occurrence, development, and intervention of depression.

Discussion

Our results provide evidence of relationships among stress, microvascular dysfunction, and depression-like behaviors (Figs. 1 and 3 and Supplementary Fig. 4). Consistently, chronic stress has been linked to increased risk for cardiovascular disease and depression, with vascular risk factors associated with heightened susceptibility to depression^{33,34}. Patients grappling with depression frequently exhibit peripheral vascular damage, such as generalized microvascular dysfunction and peripheral vascular disease³⁵. Previous studies also show that various types of chronic stress in adulthood can induce damage to microcirculation function including cerebrovascular damage in the form of scattered microbleeds caused by chronic social defeat, irreversible impaired autoregulation in murine retinal arterioles induced by chronic social defeat^{36,37}. Meanwhile, chronic

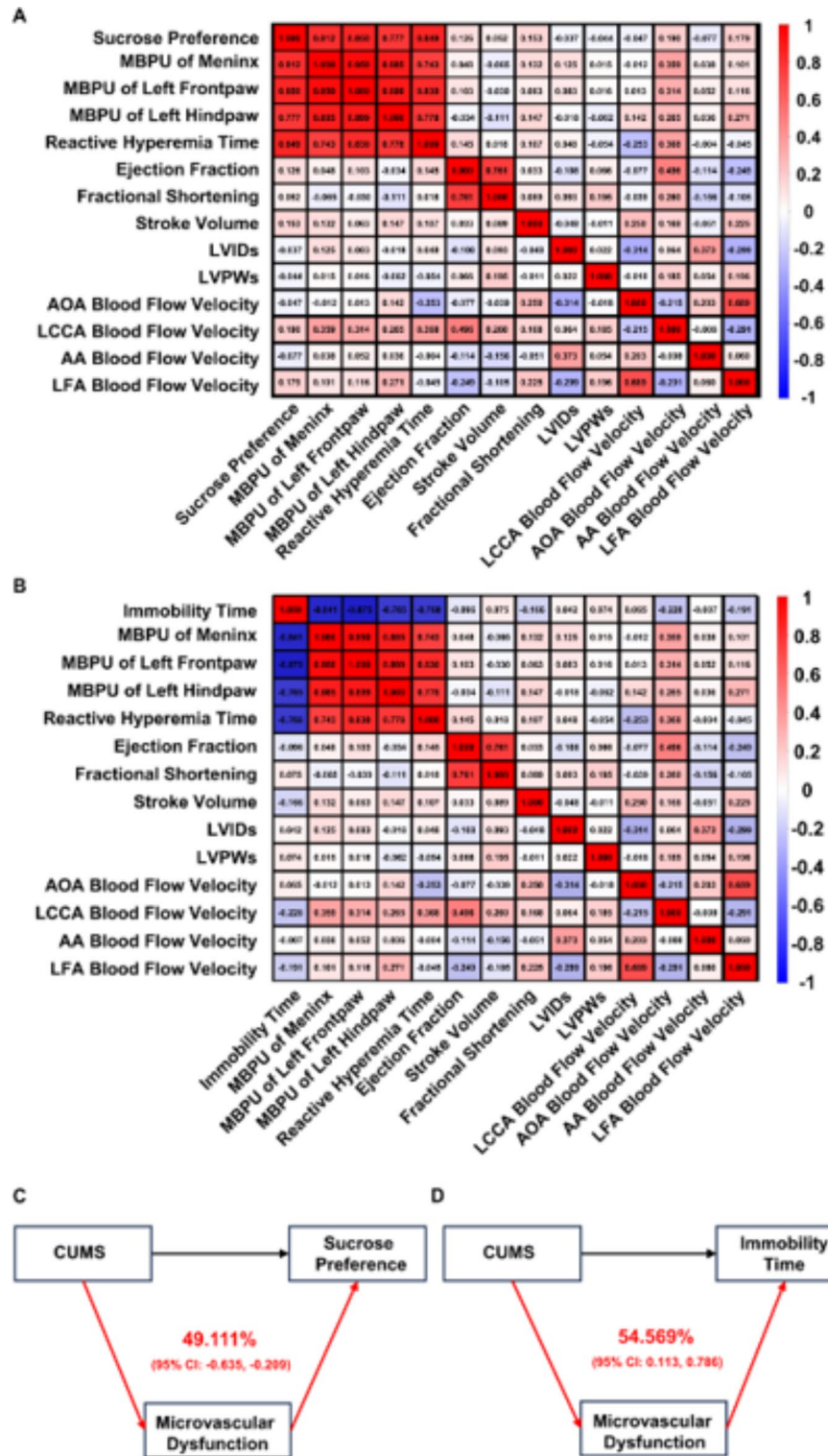


Fig. 3. Microvascular dysfunction plays a key role in the process of stress leading to depressive behavior. (A) Spearman correlation analysis of changes in the circulatory system and sucrose preference induced by CUMS. (B) Spearman correlation analysis of changes in the circulatory system and immobility time of forced swimming test induced by CUMS. (C) Mediating effect model diagram of microvascular dysfunction on the relationship between stress and sucrose preference. (D) Mediating effect model diagram of microvascular dysfunction on the relationship between stress and immobility time of forced swimming. Blue squares indicate negative correlations, white squares indicate non-applicable correlations, and red squares indicate positive correlations, the deeper the color, the stronger the trend. Absolute value greater than 0.7 was considered to indicate a correlation. $P^* < 0.05$, $P^{**} < 0.01$ vs. Control. Spearman correlation analysis, generalized linear regression analysis and mediation effect analysis were used.

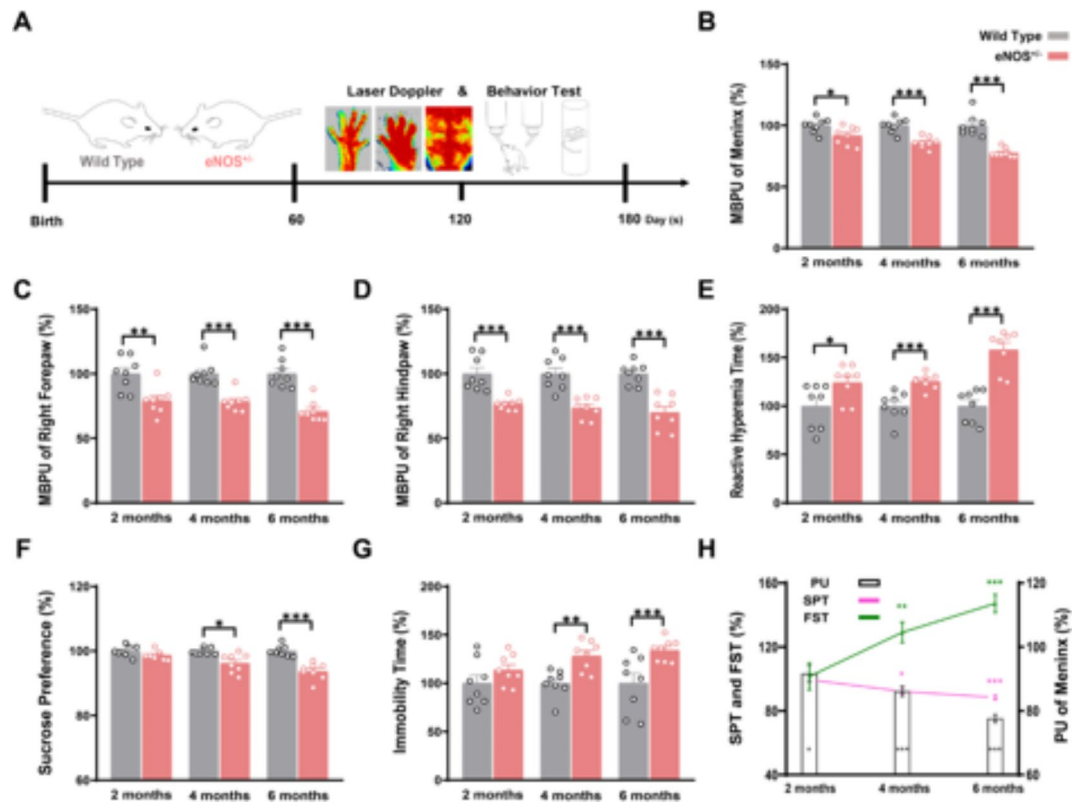


Fig. 4. Microvascular dysfunction induced by endothelial injury can cause depression-like behavior. (A) Timeline of the experiment in *eNOS*^{+/-} mice and control littermates. We selected three time periods of 2 months, 4 months, and 6 months as experimental nodes. (B) Standardized statistical results of cerebral PU in *eNOS*^{+/-} mice and WT. (C) Standardized statistical results of right forepaw PU in *eNOS*^{+/-} mice and WT. (D) Standardized statistical results of right hindpaw PU in *eNOS*^{+/-} mice and WT. (E) Standardized statistical results of PORH time in *eNOS*^{+/-} mice and WT. (F) Standardized statistical results of sucrose preference during SPT. (G) Standardized statistical results of immobility time during FST. (H) Trend plots of cerebral perfusion and depression-like behavioral. *eNOS*: endothelial nitric oxide synthase, WT: wild type littermates. WT group was used as the standard value (100%) in each group. $P^* < 0.05$, $P^{**} < 0.01$, $P^{***} < 0.001$ vs. WT.

stress can impair endothelium-dependent vasorelaxation was reported, which accelerated aortic senescence and impaired aortic endothelial sprouting^{38,39}. However, the causal relationship between microvascular dysfunction and depression remains unclear. Our study, employing mediation analysis, for the first time statistically suggests that microvascular dysfunction plays a key role in depression induced by chronic stress in adulthood (Figs. 3 and 4 and Supplementary Fig. 4). Moreover, subsequent experiments with endothelial function defect mice and rescue experiments further corroborate this causal relationship (Fig. 4 and Fig. 5). Together, our findings propose a perspective that positions depression as a systemic disease influenced by peripheral tissues through microvascular disorders. However, the above inference still requires validations by more in-depth experiments.

Compare with CUMS or CSDS, MS does not cause any microvascular dysfunction in current study (Fig. 1). We consider reasons for this discrepancy may be due to differences in stress patterns (CUMS, CSDS vs. MS), the age of the subjects (adult mice vs. new born pups) or species differences (mice vs. rats). First, chronic stress models in adulthood like CUMS and CSDS due to their variability and unpredictability of stress factors may lead to more significant microvascular dysfunction and depressive-like behaviors^{36,37}. In contrast, the stimulation by the MS protocol is milder, and does not appear to cause damage to the vascular system⁴⁰. Additionally, the nervous system was in a critical developmental period and is more sensitive to external stimuli than vascular system⁴¹. During the MS modeling, the animal's cardiovascular system was relatively mature and has a certain ability to resist external stimuli⁴², since the vascular system develops earlier than the nervous system⁴³. Besides, vascular endothelial cells are a class of cells with the ability to regenerate and repair, enabling them to self-repair vascular injuries to some extent over time⁴⁴. Meanwhile research findings indicate that there are distinct behavioral responses to maternal separation between rats⁴⁵ and mice^{46,47}. Together, these results underscore the necessity for distinct clinical intervention strategies in the treatment of depression arising from various stressors, given the disparate pathogenesis of early life stress and adult chronic stress-induced depression.

Our study provides evidence that genetic *eNOS* deficit spontaneously induces chronic microvascular dysfunction in mice, worsening with age and progressively developing into depression-like behavior Fig. 4. Similarly, several literature reports that genetic *eNOS* deficit presents significant endothelial and vascular dysfunction phenotypes by reducing *eNOS* activity and NO production, accompanied with anxiety and cognitive

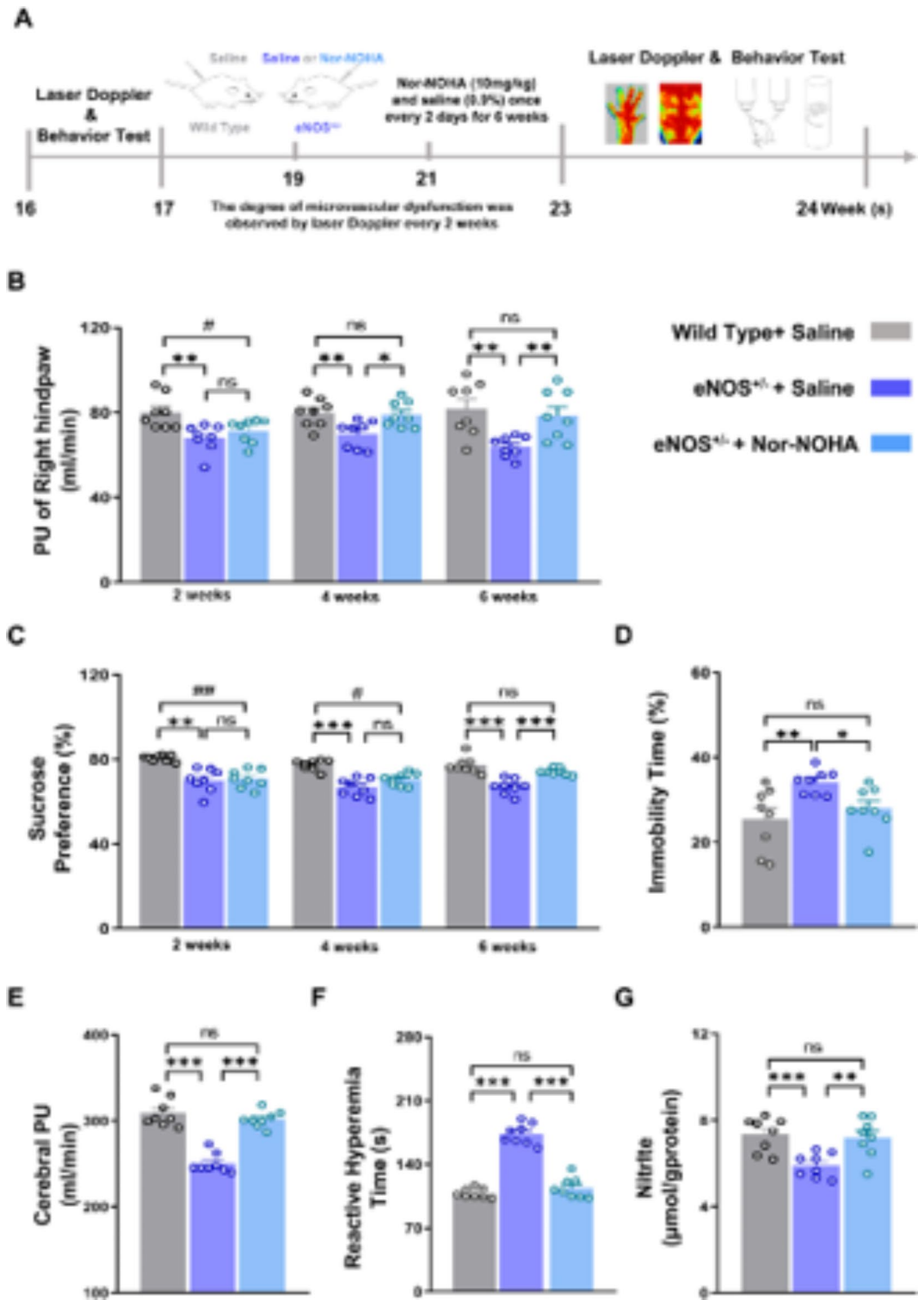


Fig. 5. Arginase inhibitors rescued microvascular dysfunction and depression-like behavior caused by endothelial injury in *eNOS*^{+/-} mice. **(A)** Timeline of drug treatment experiments in *eNOS*^{+/-} mice and WT littermates. Laser Doppler Measurement and behavioral test were performed before and 6 weeks after intraperitoneal injection of arginase inhibitor and saline from the age of 4 months. **(B)** Right hindpaw PU of *eNOS*^{+/-} mice and WT mice during treatment. **(C)** Sucrose preference during treatment. **(D)** Percentage of immobility time to total time during FST after treatment. **(E)** Cerebral PU after treatment. **(F)** Time of PORH after treatment. **(G)** Nitric oxide in brain tissue after treatment. Nor-NOHA: N-Hydroxy-nor-L-arginine Dihydrochloride, Typical arginase inhibitors. *P** < 0.05, *P*** < 0.01, *P**** < 0.001 vs. WT. *N* = 8.

decline²⁴. Consistently, as a common and early event in circulatory system damage, vascular endothelium injury was also reported in depressed patients^{48,49}. Furthermore, our findings further revealed that the increased NO production by Nor-NOHA treatment restored normal microvascular physiological function earlier than ameliorated depression-like behaviors in *eNOS*^{+/-} mice Fig. 5. This may also explain why some cardio-cerebrovascular drugs also have antidepressant effects in clinical practice. In neurodegenerative disease models like vascular dementia and Alzheimer's, enhancing neurotransmission via improved microcirculation has been implicated in therapeutic effects^{50,51}, this has yet to be explored in stress-induced depression models, warranting future mechanistic investigations. Together, these results confirm that the pivotal role of microvascular dysfunction in the onset of depression and highlight the potential applications of targeting microvascular system in the intervention of depressive patients.

In conclusion, we identified impaired microvascular function in adulthood chronic stress-induced depression in stress-induced depression-like behaviors. The improvement of microvascular dysfunction rescues depression-like behaviors in mice. These results signify microvascular injury as a critical factor in chronic stress-induced depression in adulthood, emphasizing the regulation of microvascular system function as a novel strategy for depression treatment.

Materials and methods

Animals

Male C57BL/6 mice (7–8 weeks old), male CD-1 mice (13–15 weeks old), and male as well as nulliparous female Wistar rats (8 weeks old) were obtained from Beijing Vital River Laboratory Animal Technology Co., Ltd. Male endothelial nitric oxide synthase knockout (*eNOS*^{-/-}) mice were obtained from The Jackson Laboratory (stock NO.002684). Sexually experienced retired male CD-1 breeders served as aggressors for chronic social defeat stress. Male *eNOS*^{-/-} homozygous mice were bred with wild type C57BL/6J mice to obtain the F1 generation of *eNOS*^{+/-}, which were used as experimental subjects. Animals were housed under standard specific pathogen free conditions at an appropriate temperature (22 ± 2 °C) and humidity of 60%, with a 12 h light/dark cycle. Food and water were provided ad libitum. The authors affirm that this study was carried out in accordance with the ARRIVE guidelines for reporting animal research. All animal procedures were approved by the Committee for Experimental Animal of Shandong University of Traditional Chinese Medicine under protocol number SDUTCM20230828014.

Animal models of depressive disorder

Following a 7-day adaptive feeding period, rodents with normal locomotor activity, as assessed by their movement patterns and activity levels in the open field test, were selected for further experiments.

Chronic unpredictable mild stress (CUMS)

The CUMS model was conducted as previously described with slight modifications⁵². Mice were housed individually and subjected to a variety of stressors, including: (1) cold swim at 4 °C for 10 min; (2) 24-hour food deprivation; (3) cage tilting for 12 h; (4) tail pinching for 10 min; (5) 24-hour reversal of the light/dark cycle; (6) 24-hour exposure to a wet pad; (7) restraint stress for 4 h; (8) shaky cage 1 time/s for 15 min; (9) no bedding for 24 h. These stressors were applied randomly, twice daily, for a duration of 4 weeks. One day after the final stress session, depression-like behavior was assessed using the open-field test (OFT), sucrose preference test (SPT), and forced swimming test (FST).

Chronic social defeat stress (CSDS)

The CSDS model was carried out as previously reported with minor modifications⁵². C57BL/6J mice were exposed to daily 10-minute confrontations with different CD1 aggressive counterparts. Following each confrontation, the mice were placed in non-contact isolation for a 24-hour period. This protocol was conducted over a 10-day period, with each experimental mouse encountering a unique CD1 aggressor each day. The day after the stress regimen concluded, mice exhibiting susceptibility to stress were identified using the Social Interaction Test (SIT) for subsequent experimentation (Supplementary Fig. 1A and B). Behavioral tests, including the OFT, SPT, and FST, were used to observe depression-like behavior.

Maternal separation (MS)

Maternal separation (MS) experiments were conducted daily from postnatal day 1 (PD1) to postnatal day 21 (PD21). Between the hours of 09:00 and 13:00 each day, the adult rats were removed from their home cages and placed in separate cages, while the pups remained in their original environment. The control group rats and their offspring were left undisturbed throughout this period until weaning. On PD21, all pups were weaned and subsequently grouped into new cages, with four to five pups per cage, until they reached two months of age. Female offspring were excluded from further analysis⁵³. Behavioral testing to observe depression-like behavior in rats was conducted after postnatal day 60 (PD60), using OFT, SPT and FST.

Behavioral tests

Open-field test (OFT)

An open activity box (mice: 50 cm x 50 cm x 40 cm, rat: 80 cm x 80 cm x 40 cm) was placed on an open floor with a camera mounted at the center above the box. Animals were conditioned in the test room for 2 h in advance. Subsequently, each animal was carefully positioned at the center of the chamber and permitted to explore the space without restriction for a duration of 15 min. The total distance travelled in the box and the time spent in the center were recorded by the camera. The box was cleaned with 20% ethanol between sessions⁵⁴. Data were recorded using VisuTrack software (Shanghai Xinruan Software Technology Co., Ltd.).

Sucrose preference test (SPT)

To uniformly evaluate different model animals, all behavioral test methods were adapted from our previous study⁵³. Anhedonic responses were assessed using a standard sucrose preference test. Water bottles in the cages were removed and replaced with two 50 mL conical tubes with sipper tops, filled with water, for a 24-hour habituation period. After 24 h, water in both the 50 mL conical tubes was replaced with a 1% sucrose solution for another 24 h habituation period. Subsequently, one of the 50 mL conical tubes containing 1% sucrose solution was replaced with water for the formal experiment. Animals had ad libitum access to the solutions for a 12-hour period. After consumption, the tubes were reweighed and then alternated to prevent location bias during the subsequent 12-hour drinking period. At the end of the 24-hour test, sucrose preference was calculated by dividing the total volume of sucrose solution consumed by the total fluid intake during the 24-hour sucrose exposure period.

Forced swimming test (FST)

Animals were transported to the laboratory and placed in a transparent plastic cylinder (25 cm * 10 cm for mice and 40 cm * 20 cm for rats), filled with 20–30 cm of water at a temperature ranging from 22 °C to 24 °C, respectively. The test duration was 6 min, during which the animals' immobility was recorded. Immobility was defined as the lack of movement for more than 10 s. Following the test, the animals were dried with paper towels⁵⁵. The duration of immobility was recorded by VisuTrack (Shanghai Xinruan Software Technology Co., Ltd.).

Social interaction test (SIT)

The Social Interaction Test was conducted one day after the last stress session in an open activity box (50 cm x 50 cm x 40 cm). The test consists of two parts. Initially, a 24 × 14 cm area was designated as the social contact zone on one side of the open box. A small compartment (8 × 6 cm) was partitioned from the social contact area by a transparent plastic spacer to prevent direct contact with CD1 mice. The spacer contained small holes that allowed C57BL/6J mice to detect the presence of the unfamiliar CD1 mice. Next, in the absence of CD1 mice in the compartment (target absent phase), the C57BL/6J mice were placed in the central area of the open box and allowed to move freely for 2.5 min. Their frequency of entering the social interaction zone was recorded during this period. The open box was cleaned after the first part of the test. In the second part of the test (target present stage), an unfamiliar CD1 mouse, which had no prior contact with the C57BL/6J mice, was placed in the compartment. The C57BL/6J mice were then returned to the open box, and the number of times they entered the social contact area was recorded over 2.5 min. The social interaction ratio (SI ratio) for each C57BL/6J mouse was calculated as follows: SI ratio = target time (in interaction zone)/no target time (in interaction zone). Data were recorded using VisuTrack (Shanghai Xinruan Software Technology Co., Ltd.). Based on the time spent in the interaction zone and the social interaction ratio, the experimental mice subjected to CSDS stress could be preliminarily categorized. Mice with an SI ratio less than 1 were classified as stress-sensitive, while those with an SI ratio greater than 1 were considered stress-resistant⁵⁶.

Laser Doppler measurement

Following the methodology established in our previous study 引文, we assessed in vivo microvascular perfusion in the meninges, the right forepaw, and the right hindpaw using laser Doppler flowmetry (PERIMED PeriFlux5000 system, Sweden). Animals were anesthetized with 1.5% (mice) or 1% (rat) isoflurane and placed on a heating pad to maintain body temperature. The hair on the plantar surfaces of the regions of interest (ROI) was gently removed using hair removal cream, and the surfaces were then positioned on a dark surgical towel. The mean Perfusion Unit (PU) was recorded, with the laser scan head optimized for optimal image quality and a constant distance maintained for all measurements. Baseline blood flow measurements were taken over a 2-minute scan duration. To measure peripheral reactive hyperemic responses (PORH), stable PU values of the hind limbs were established as the resting blood flow. The right hind limbs were then clamped to induce a blood flow block, confirmed by zero perfusion. After 30 s of ischemia, the pressure was released, and the time taken for the PU value to return from 0 to the resting blood flow value was recorded as the reactive hyperemia time of the hind limbs. The total or average flow, expressed in PU, was automatically calculated by summing the pixel values within the manually outlined hind limbs region. The mean flow in this region was computed by the software provided by the manufacturer^{57,58}.

In vivo ultrasound imaging and assessment

The in vivo ultrasound imaging method was adapted from our previous study⁵⁷. Cardiac function and hemodynamic function in the carotid, arcus aortae, abdominal aorta and femoral arteries were evaluated using a SiliconWave 60 Ultrasound Image system (KOLO, China), with a frequency range of 22–38 MHz and a central frequency of 30 MHz. Measurements were obtained randomly and labeled by a single operator. Animals were anesthetized with 2% (mice) or 4% (rat) isoflurane in a chamber with 1 L/min of medical oxygen for 3–5 min, after which the isoflurane concentration was reduced to 1.5% (for mice) or 1% (for rats) to maintain anesthesia during imaging. The animals were positioned supinely, and hair on the neck, chest, abdomen, and legs was removed using depilatory cream to facilitate imaging while controlling body temperature. The probe was positioned parallel to the animal's neck to locate the left carotid arteries, and M-mode images were used to measure blood flow velocity in the left common carotid arteries (LCCA) during contraction. The probe was then moved to the chest to locate the ventricular center, and M-mode images were used to measure cardiac function and systolic blood flow velocity (AOA) of the aortic arch. Subsequently, the probe was moved to the abdomen to locate the abdominal aorta (AA) and to the calf to locate the left femoral artery (LFA) to measure blood

flow velocity during contraction of the AA and LFA, respectively. The results were recorded using the Off-line Workstation package (WS01, KOLO, China).

Mediation analysis

To examine the correlation between circulatory damage and stress-induced depressive disorder, we employed Spearman correlation analysis. Heatmap cluster analysis was used to determine the relationship between 13 evaluation indicators of circulatory damage and 2 evaluation indicators of depression⁵⁹. We selected significant evaluation indicators ($P \leq 0.05$) from the Spearman analysis as candidates for mediation analysis. Due to the complexity of assessing microvascular injury, reliance on a single indicator would not adequately capture systemic damage, and assigning weights based on previous studies is challenging. Therefore, we applied the common objective weighting method, specifically the entropy weighting method, to calculate the weight of each microvascular damage indicator, providing a foundation for a multi-index comprehensive evaluation of microvascular damage (detailed weight values are shown in Supplementary Tables 1–4). As we focused solely on circulation and excluded other interfering factors in this study, we used the classical mediation analysis method. We constructed a structural equation model based on statistical results, performed mediation effect testing using the bootstrap method, and conducted group path analysis with a sampling frequency of 5000. A P-value of ≤ 0.05 was considered statistically significant⁶⁰. The detailed process of mediation analysis is provided in Supplementary Tables 1–4.

Replenish with nitric oxide

eNOS^{+/-} mice received intraperitoneal injections of the arginase inhibitor Nor-NOHA (10 mg/kg, dissolve in saline, monacetate, 93555, MCE) every 2 days for a total of 6 weeks. Concurrently, littermate wild-type and *eNOS*^{+/-} control mice were administered saline injections^{61,62}. The blood perfusion of the right hind paw was measured every 2 weeks, SPT and FST were performed after the blood perfusion of the right hindpaw no longer showed a significant decrease compared to littermate control mice.

Total NO production assay

The Total NO Assay Kit (S0023, Beyotime, China) and the Griess reagent were used to assess total NO production. Due to the rapid metabolism of NO to Nitrate and Nitrite, total NO production was evaluated by determining nitrite content after converting nitrate to nitrite using nitrate reductase. Briefly, 60 μ L of each brain sample supernatant was incubated with 5 μ L of nicotinamide adenine dinucleotide phosphate, 10 μ L of flavin adenine dinucleotide and 5 μ L of nitrate reductase for 30 min at 37 °C. Then, 10 μ L of lactate dehydrogenase buffer and 10 μ L of LDH were added in the above reaction buffer for an additional 30 min at 37 °C. Finally, 50 μ L of Griess reagent I and 50 μ L of Griess reagent II were mixed into all the above wells before incubation for 10 min. The optical density at 540 nm was measured using a microplate reader (Multiskan SkyHigh, Thermo Scientific, USA). Concentrations were determined by comparing the absorbance to a standard curve⁶³.

Statistics

Data analyses and visualizations were conducted using SPSS 21.0 (Chicago, IL, USA) and GraphPad Prism version 8.0 (San Diego, CA, USA). All data are represented as mean \pm SEM. Statistical differences were evaluated using unpaired t test. The blank control group for each model was set as the reference, with its value considered as 100%. The relative change values for each model or transgenic animal were then calculated individually. Specific values for control animals in the various groups are detailed in Supplementary Tables 5 and 6. The number of animals is denoted by “n”, and a p-value of ≤ 0.05 was deemed statistically significant, indicating a significant difference.

Data availability

All data generated or analysed during this study are included in this published article (and its Supplementary Information files).

Received: 25 June 2024; Accepted: 30 September 2024

Published online: 14 October 2024

References

1. Malhi, G. S. & Mann, J. J. Depression. *Lancet* **392**, 2299–2312. [https://doi.org/10.1016/s0140-6736\(18\)31948-2](https://doi.org/10.1016/s0140-6736(18)31948-2) (2018).
2. Amick, H. R. et al. Comparative benefits and harms of second generation antidepressants and cognitive behavioral therapies in initial treatment of major depressive disorder: Systematic review and meta-analysis. *BMJ* **351**, h6019. <https://doi.org/10.1136/bmj.h6019> (2015).
3. Talati, A. Maternal depression, prenatal SSRI exposure, and brain trajectories in childhood. *JAMA Psychiat.* **80**, 1191–1192. <https://doi.org/10.1001/jamapsychiatry.2023.2664> (2023).
4. Smith-Apeldoorn, S. Y., Veraart, J. K., Spijker, J., Kamphuis, J. & Schoevers, R. A. Maintenance ketamine treatment for depression: A systematic review of efficacy, safety, and tolerability. *Lancet Psychiatry* **9**, 907–921. [https://doi.org/10.1016/s2215-0366\(22\)00317-0](https://doi.org/10.1016/s2215-0366(22)00317-0) (2022).
5. Marwaha, S. et al. Novel and emerging treatments for major depression. *Lancet* **401**, 141–153. [https://doi.org/10.1016/s0140-6736\(22\)02080-3](https://doi.org/10.1016/s0140-6736(22)02080-3) (2023).
6. van Agtmaal, M. J. M., Houben, A., Pouwer, F., Stehouwer, C. D. A. & Schram, M. T. Association of microvascular dysfunction with late-life depression: A systematic review and meta-analysis. *JAMA Psychiat.* **74**, 729–739. <https://doi.org/10.1001/jamapsychiatry.2017.0984> (2017).
7. Wang, L., Xiong, X., Zhang, L. & Shen, J. Neurovascular unit: A critical role in ischemic stroke. *CNS Neurosci. Therap.* **27**, 7–16. <https://doi.org/10.1111/cns.13561> (2021).

8. Greaney, J. L., Koffer, R. E., Saunders, E. F. H., Almeida, D. M. & Alexander, L. M. Self-reported everyday psychosocial stressors are associated with greater impairments in endothelial function in young adults with major depressive disorder. *J. Am. Heart Assoc.* **8**, e010825. <https://doi.org/10.1161/jaha.118.010825> (2019).
9. Cooper, C. M. et al. Discovery and replication of cerebral blood flow differences in major depressive disorder. *Mol. Psychiatry* **25**, 1500–1510. <https://doi.org/10.1038/s41380-019-0464-7> (2020).
10. Tao, S. H., Ren, X. Q., Zhang, L. J. & Liu, M. Y. Association between common cardiovascular drugs and depression. *Chin. Med. J.* **134**, 2656–2665. <https://doi.org/10.1097/cm9.0000000000001875> (2021).
11. Matsuno, H. et al. Association between vascular endothelial growth factor-mediated blood-brain barrier dysfunction and stress-induced depression. *Mol. Psychiatry* **27**, 3822–3832. <https://doi.org/10.1038/s41380-022-01618-3> (2022).
12. Ingrini, E., Belzung, C., d'Audiffret, A. & Camus, V. Early and late-onset effect of chronic stress on vascular function in mice: A possible model of the impact of depression on vascular disease in aging. *Am. J. Geriatr. Psychiatry* **19**, 335–346. <https://doi.org/10.1097/JGP.0b013e318202bc42> (2011).
13. Iadecola, C. The neurovascular unit coming of age: A journey through neurovascular coupling in health and disease. *Neuron* **96**, 17–42. <https://doi.org/10.1016/j.neuron.2017.07.030> (2017).
14. Wang, W. et al. Endothelial cells mediated by UCP2 control the neurogenic-to-astrogenic neural stem cells fate switch during brain development. *Adv. Sci.* **9**, e2105208. <https://doi.org/10.1002/adv.202105208> (2022).
15. Cyr, A. R., Huckaby, L. V., Shiva, S. S. & Zuckerbraun, B. S. Nitric oxide and endothelial dysfunction. *Crit. Care Clin.* **36**, 307–321. <https://doi.org/10.1016/j.ccc.2019.12.009> (2020).
16. Zhu, H. Y., Hong, F. F. & Yang, S. L. The roles of nitric oxide synthase/nitric oxide pathway in the pathology of vascular dementia and related therapeutic approaches. *Int. J. Mol. Sci.* **22**. <https://doi.org/10.3390/ijms22094540> (2021).
17. Ahmed, S. et al. Partial endothelial nitric oxide synthase deficiency exacerbates cognitive deficit and amyloid pathology in the APP^{swe}/PS1^{ΔE9} mouse model of Alzheimer's disease. *Int. J. Mol. Sci.* **23**. <https://doi.org/10.3390/ijms23137316> (2022).
18. Chen, A. Q. et al. Microglia-derived TNF- α mediates endothelial necroptosis aggravating blood brain-barrier disruption after ischemic stroke. *Cell Death Dis.* **10**, 487. <https://doi.org/10.1038/s41419-019-1716-9> (2019).
19. Chrapko, W. E. et al. Decreased platelet nitric oxide synthase activity and plasma nitric oxide metabolites in major depressive disorder. *Biol. Psychiatry* **56**, 129–134. <https://doi.org/10.1016/j.biopsych.2004.03.003> (2004).
20. Liao, F. F. et al. Endothelial nitric oxide synthase-deficient mice: A model of spontaneous cerebral small-vessel disease. *Am. J. Pathol.* **191**, 1932–1945. <https://doi.org/10.1016/j.ajpath.2021.02.022> (2021).
21. Mohan, S. et al. Diabetic eNOS knockout mice develop distinct macro- and microvascular complications. *Lab. Invest.* **88**, 515–528. <https://doi.org/10.1038/labinvest.2008.23> (2008).
22. Ma, L. et al. SGLT2 inhibitor dapagliflozin reduces endothelial dysfunction and microvascular damage during cardiac ischemia/reperfusion injury through normalizing the XO-SERCA2-CaMKII-cofilin pathways. *Theranostics* **12**, 5034–5050. <https://doi.org/10.7150/thno.75121> (2022).
23. Bloom, S. I., Islam, M. T., Lesniewski, L. A. & Donato, A. J. Mechanisms and consequences of endothelial cell senescence. *Nat. Rev. Cardiol.* **20**, 38–51. <https://doi.org/10.1038/s41569-022-00739-0> (2023).
24. Tan, X. L. et al. Partial eNOS deficiency causes spontaneous thrombotic cerebral infarction, amyloid angiopathy and cognitive impairment. *Mol. Neurodegener.* **10**, 24. <https://doi.org/10.1186/s13024-015-0020-0> (2015).
25. Monroe, S. M. & Harkness, K. L. Major Depression and Its Recurrences: Life Course Matters. *Annu. Rev. Clin. Psychol.* **18**, 329–357. <https://doi.org/10.1146/annurev-clinpsy-072220-021440> (2022).
26. Martin, E. A. et al. Sex differences in vascular and endothelial responses to acute mental stress. *Clin. Autonomic Res.* **18**, 339–345. <https://doi.org/10.1007/s10286-008-0497-5> (2008).
27. Gururajan, A., Reif, A., Cryan, J. F. & Slattery, D. A. The future of rodent models in depression research. *Nature reviews. Neuroscience* **20**, 686–701. <https://doi.org/10.1038/s41583-019-0221-6> (2019).
28. Kivimäki, M. & Steptoe, A. Effects of stress on the development and progression of cardiovascular disease. *Nat. Rev. Cardiol.* **15**, 215–229. <https://doi.org/10.1038/nrcardio.2017.189> (2018).
29. Xia, N. & Li, H. Loneliness, Social Isolation, and Cardiovascular Health. *Antioxid. Redox Signal.* **28**, 837–851. <https://doi.org/10.1089/ars.2017.7312> (2018).
30. Osborne, M. T. et al. Disentangling the links between psychosocial stress and cardiovascular disease. *Circ. Cardiovasc. Imaging* **13**, e010931. <https://doi.org/10.1161/circimaging.120.010931> (2020).
31. Lurbe, E. & Ingelfinger, J. Developmental and early life origins of cardiometabolic risk factors: Novel findings and implications. *Hypertension* **77**, 308–318. <https://doi.org/10.1161/hypertensionaha.120.14592> (2021).
32. Garcia, V. & Sessa, W. C. Endothelial NOS: Perspective and recent developments. *Brit. J. Pharmacol.* **176**, 189–196. <https://doi.org/10.1111/bph.14522> (2019).
33. Ayerbe, L. et al. Disparities in the management of cardiovascular risk factors in patients with psychiatric disorders: A systematic review and meta-analysis. *Psychol. Med.* **48**, 2693–2701. <https://doi.org/10.1017/s0033291718000302> (2018).
34. Chaplin, A. B. et al. Longitudinal association between cardiovascular risk factors and depression in young people: A systematic review and meta-analysis of cohort studies. *Psychol. Med.* **53**, 1049–1059. <https://doi.org/10.1017/s0033291721002488> (2023).
35. Daskalopoulou, M. et al. Depression as a risk factor for the initial presentation of twelve cardiac, cerebrovascular, and peripheral arterial diseases: Data linkage study of 1.9 million women and men. *PLoS ONE* **11**, e0153838. <https://doi.org/10.1371/journal.pone.0153838> (2016).
36. Samuels, J. D. et al. Chronic social defeat alters brain vascular-associated cell gene expression patterns leading to vascular dysfunction and immune system activation. *J. Neuroinflamm.* **20**, 154. <https://doi.org/10.1186/s12974-023-02827-5> (2023).
37. Wang, M. et al. Chronic social defeat stress causes retinal vascular dysfunction. *Exp. Eye Res.* **213**, 108853. <https://doi.org/10.1016/j.exer.2021.108853> (2021).
38. Balkaya, M. et al. Stress worsens endothelial function and ischemic stroke via glucocorticoids. *Stroke* **42**, 3258–3264. <https://doi.org/10.1161/strokeaha.110.607705> (2011).
39. Piao, L. et al. Chronic psychological stress accelerates vascular senescence and impairs ischemia-induced neovascularization: The role of dipeptidyl peptidase-4/Glucagon-like peptide-1-adiponectin axis. *J. Am. Heart Assoc.* **6**. <https://doi.org/10.1161/jaha.117.006421> (2017).
40. Zhang, Y. et al. Comparison of the chronic unpredictable mild stress and the maternal separation in mice postpartum depression modeling. *Biochem. Biophys. Res. Commun.* **632**, 24–31. <https://doi.org/10.1016/j.bbrc.2022.09.063> (2022).
41. Hogan, M. K., Hamilton, G. F. & Horner, P. J. Neural stimulation and molecular mechanisms of plasticity and regeneration: A review. *Front. Cell. Neurosci.* **14**, 271. <https://doi.org/10.3389/fncel.2020.00271> (2020).
42. Sanders, B. J. & Anticevic, A. Maternal separation enhances neuronal activation and cardiovascular responses to acute stress in borderline hypertensive rats. *Behav. Brain Res.* **183**, 25–30. <https://doi.org/10.1016/j.bbr.2007.05.020> (2007).
43. Vogenstahl, J., Parrilla, M., Acker-Palmer, A. & Segarra, M. Vascular regulation of developmental neurogenesis. *Front. Cell Dev. Biol.* **10**, 890852. <https://doi.org/10.3389/fcell.2022.890852> (2022).
44. Rust, R., Grönnert, L., Weber, R. Z., Mulders, G. & Schwab, M. E. Refueling the ischemic CNS: Guidance molecules for vascular repair. *Trends Neurosci.* **42**, 644–656. <https://doi.org/10.1016/j.tins.2019.05.006> (2019).
45. Matthews, K. & Robbins, T. W. Early experience as a determinant of adult behavioural responses to reward: The effects of repeated maternal separation in the rat. *Neurosci. Biobehav. Rev.* **27**, 45–55. [https://doi.org/10.1016/s0149-7634\(03\)00008-3](https://doi.org/10.1016/s0149-7634(03)00008-3) (2003).

46. Shin, S. & Lee, S. The impact of environmental factors during maternal separation on the behaviors of adolescent C57BL/6 mice. *Front. Mol. Neurosci.* **16**, 1147951. <https://doi.org/10.3389/fnmol.2023.1147951> (2023).
47. Millstein, R. A. & Holmes, A. Effects of repeated maternal separation on anxiety- and depression-related phenotypes in different mouse strains. *Neurosci. Biobehav. Rev.* **31**, 3–17. <https://doi.org/10.1016/j.neubiorev.2006.05.003> (2007).
48. Liu, M. Y., Li, N., Li, W. A. & Khan, H. Association between psychosocial stress and hypertension: A systematic review and meta-analysis. *Neurol. Res.* **39**, 573–580. <https://doi.org/10.1080/01616412.2017.1317904> (2017).
49. Wacławowski, A. J. et al. Endothelial dysfunction in people with depressive disorders: A systematic review and meta-analysis. *J. Psychiatric Res.* **141**, 152–159. <https://doi.org/10.1016/j.jpsychires.2021.06.045> (2021).
50. Tarantini, S. et al. Nicotinamide mononucleotide (NMN) supplementation rescues cerebrovascular endothelial function and neurovascular coupling responses and improves cognitive function in aged mice. *Redox Biol.* **24**, 101192. <https://doi.org/10.1016/j.redox.2019.101192> (2019).
51. Zhai, Y. et al. Chronic cerebral hypoperfusion accelerates Alzheimer's disease pathology with cerebrovascular remodeling in a novel mouse model. *J. Alzheimer's Dis.* **53**, 893–905. <https://doi.org/10.3233/jad-160345> (2016).
52. Song, A. Q. et al. NLRP1 inflammasome contributes to chronic stress-induced depressive-like behaviors in mice. *J. Neuroinflamm.* **17**, 178. <https://doi.org/10.1186/s12974-020-01848-8> (2020).
53. Zheng, Y. et al. Electroacupuncture-modulated extracellular ATP levels in prefrontal cortex ameliorated depressive-like behavior of maternal separation rats. *Behav. Brain Res.* **452**, 114548. <https://doi.org/10.1016/j.bbr.2023.114548> (2023).
54. Brooks, S. P. & Dunnett, S. B. Tests to assess motor phenotype in mice: A user's guide. *Nat. Rev. Neurosci.* **10**, 519–529. <https://doi.org/10.1038/nrn2652> (2009).
55. Armario, A. The forced swim test: Historical, conceptual and methodological considerations and its relationship with individual behavioral traits. *Neurosci. Biobehav. Rev.* **128**, 74–86. <https://doi.org/10.1016/j.neubiorev.2021.06.014> (2021).
56. Golden, S. A., Covington, H. E. 3rd., Berton, O. & Russo, S. J. A standardized protocol for repeated social defeat stress in mice. *Nat. Protoc.* **6**, 1183–1191. <https://doi.org/10.1038/nprot.2011.361> (2011).
57. Wang, J. et al. Modulating activity of PVN neurons prevents atrial fibrillation induced circulation dysfunction by electroacupuncture at BL15. *Chin. Med.* **18**, 135. <https://doi.org/10.1186/s13020-023-00841-6> (2023).
58. Chen, M. et al. The activation of histone deacetylases 4 prevented endothelial dysfunction: A crucial mechanism of HuangqiGuizhiWuwu decoction in improving microcirculation dysfunction in diabetes. *J. Ethnopharmacol.* **307**, 116240. <https://doi.org/10.1016/j.jep.2023.116240> (2023).
59. Saeed, O. et al. Investigating the impacts of heavy metal(loid)s on ecology and human health in the lower basin of Hungary's Danube River: A python and Monte Carlo simulation-based study. *Environ. Geochem. Health* **45**, 9757–9784. <https://doi.org/10.1007/s10653-023-01769-4> (2023).
60. Luo, Z. et al. Establishment of an indicator framework for the transmission risk of the mountain-type zoonotic visceral leishmaniasis based on the Delphi-entropy weight method. *Infect. Dis. Poverty* **11**, 122. <https://doi.org/10.1186/s40249-022-01045-0> (2022).
61. Brandt, A. et al. Impairments of intestinal arginine and NO metabolisms trigger aging-associated intestinal barrier dysfunction and “inflammaging”. *Redox Biol.* **58**, 102528. <https://doi.org/10.1016/j.redox.2022.102528> (2022).
62. Leo, F. et al. Red blood cell and endothelial eNOS independently regulate circulating nitric oxide metabolites and blood pressure. *Circulation* **144**, 870–889. <https://doi.org/10.1161/circulationaha.120.049606> (2021).
63. Yin, C. Y. et al. Neuronal nitric oxide synthase in nucleus accumbens specifically mediates susceptibility to social defeat stress through cyclin-dependent kinase 5. *J. Neurosci.* **41**, 2523–2539. <https://doi.org/10.1523/jneurosci.0422-20.2021> (2021).

Acknowledgements

The present study was supported by the National Natural Science Foundation of China (82274128, and 82374586), the Natural Science Foundation of Shandong Province (ZR2021LZY020, and R2022QH083), the Shanghai Traditional Chinese Medicine Science and Technology Plan (Grant No. 2022CX004), the Key Laboratory of Traditional Chinese Medicine Classical Theory, Ministry of Education, Shandong University of Traditional Chinese Medicine, Jinan 250355, PR China, and the Shandong Province Chinese Medicine High-level Talents Cultivation Program Special Funds.

Author contributions

All authors participated in data acquisition. YJC and LY contributed to the conception and design of the study. XCZ, YRW, SX, LG, JLY and YJZ did the data collection and analysis. XCZ, YRW, YJF, XYY and KZH performed experiments. XCZ, YJC and LY contributed to the drafting and revision of the manuscript. All authors read and approved the final manuscript.

Declarations

Competing interests

The authors declare no competing interests.

Additional information

Supplementary Information The online version contains supplementary material available at <https://doi.org/10.1038/s41598-024-74902-7>.

Correspondence and requests for materials should be addressed to Y.C. or L.Y.

Reprints and permissions information is available at www.nature.com/reprints.

Publisher's note Springer Nature remains neutral with regard to jurisdictional claims in published maps and institutional affiliations.

Open Access This article is licensed under a Creative Commons Attribution-NonCommercial-NoDerivatives 4.0 International License, which permits any non-commercial use, sharing, distribution and reproduction in any medium or format, as long as you give appropriate credit to the original author(s) and the source, provide a link to the Creative Commons licence, and indicate if you modified the licensed material. You do not have permission under this licence to share adapted material derived from this article or parts of it. The images or other third party material in this article are included in the article's Creative Commons licence, unless indicated otherwise in a credit line to the material. If material is not included in the article's Creative Commons licence and your intended use is not permitted by statutory regulation or exceeds the permitted use, you will need to obtain permission directly from the copyright holder. To view a copy of this licence, visit <http://creativecommons.org/licenses/by-nc-nd/4.0/>.

© The Author(s) 2024